

Rotating Neutron Stars in a Chiral SU(3) Model

S. Schramm*

Argonne National Laboratory, 9700 S. Cass Avenue, Argonne IL 60439, USA

D. Zschesche

Institut für Theoretische Physik, Postfach 11 19 32,

D-60054 Frankfurt am Main, Germany

(Dated: October 28, 2018)

Abstract

We study the properties of rotating neutron stars within a generalized chiral SU(3)-flavor model. The influence of the rotation on the inner structure and the hyperon matter content of the star is discussed. We calculate the Kepler frequency and moments of inertia of the neutron star sequences. An estimate for the braking index of the associated pulsars is given.

*Electronic address: schramm@theory.phy.anl.gov

I. INTRODUCTION

Neutron stars belong to the most important physical systems where strong interactions are “tested” at extreme dense conditions. In contrast to ultrarelativistic heavy-ion collisions where also high baryonic densities might be obtained by choosing the appropriate bombarding energy, neutron star matter exists at practically zero temperature - at least on a hadronic scale. Thus the understanding of neutron stars is the complementary task of what lattice gauge calculations can achieve for high-temperature, zero-density matter. In addition due to the fact that charge neutrality drives the stellar matter away from isospin-symmetric nuclear matter the study of neutron stars can give important clues for understanding the isospin-dependence of nuclear forces. A related regime of strong interactions can be experimentally investigated using secondary beams of nuclei going towards the neutron drip-line of nuclei.

Compared to the harder task of determining masses or radii the most easily observable property of a neutron star is its rotational frequency through its pulsar radio signals emitted from the magnetic poles of the star[2]. Additional information can be obtained by the slow change of the pulsar frequency of an isolated neutron star with time signalling the slowing down of the rotation due to radiative loss of angular momentum. So far observational data in this respect are still scarce[3, 4, 5, 6].

Various hadronic models have been used to describe the structure of neutron stars. Going to central densities of a few times nuclear matter saturation density the inclusion of hyperon degrees become essential [1]. As it always will be difficult to get clear and unambiguous information on the stellar interior from the relatively limited observational data it is important to relate star properties with other observables like neutron distribution radii in neutron-rich nuclei or multi-fragmentation in heavy-ion collisions with different N/Z nuclei. It is therefore very useful to implement a model with a broader applicability including nuclear matter, finite nuclei and chiral symmetry restoration to be able to simultaneously study different observables within a unified approach using the same set of parameters for all calculations. In this paper we follow this direction by adopting a hadronic model incorporating the underlying $SU_L(3) \times SU_R(3)$ structure of QCD, which we used in earlier studies of non-rotating neutron stars, nuclear matter and finite nuclei/hypernuclei calculations [7, 8, 9].

Here we extend the static calculation to study the properties of rotating neutron (hyper-)

stars within the same approach. The outline of the article is as follows. First we give a brief description of the ingredients of the hadronic model that we implement in our calculations (a much more detailed discussion can be found in [10]). After introducing the Tolman-Oppenheimer-Volkov (TOV) equations for the static star we present the extension to rotating stars following the treatment of Hartle and Thorne [12]. In the third section we present some general features of the equation of state and its strange matter contributions and then look at the composition and gross properties of the rotating stars. We conclude with an outlook of possible extensions of the current approach.

II. THE CHIRAL MODEL

The chiral hadronic SU(3) lagrangian has the following basic structure

$$\mathcal{L} = \mathcal{L}_{\text{kin}} + \mathcal{L}_{\text{BM}} + \mathcal{L}_{\text{BV}} + \mathcal{L}_{\text{vec}} + \mathcal{L}_0 + \mathcal{L}_{\text{SB}} + \mathcal{L}_{\text{lep}} , \quad (1)$$

consisting of interaction terms between baryons and spin-0 (BM) and spin-1 (BV) mesons

$$\begin{aligned} \mathcal{L}_{\text{BM}} + \mathcal{L}_{\text{BV}} &= - \sum_i \bar{\psi}_i \left[g_{i\sigma} \sigma + g_{i\zeta} \zeta + g_{i\omega} \gamma_0 \omega^0 + g_{i\phi} \gamma_0 \phi^0 + g_{N\rho} \gamma_0 \tau_3 \rho_0 \right] \psi_i , \\ \mathcal{L}_{\text{vec}} &= \frac{1}{2} m_\omega^2 \frac{\chi^2}{\chi_0^2} \omega^2 + \frac{1}{2} m_\phi^2 \frac{\chi^2}{\chi_0^2} \phi^2 + \frac{1}{2} \frac{\chi^2}{\chi_0^2} m_\rho^2 \rho^2 + g_4^4 (\omega^4 + 2\phi^4 + 6\omega^2 \rho^2 + \rho^4) \end{aligned} \quad (2)$$

summing over the baryonic octet, (p,n, $\Sigma^{-/0/+}$, $\Xi^{-/0}$), as well as interactions between the scalar mesons

$$\begin{aligned} \mathcal{L}_0 &= -\frac{1}{2} k_0 \chi^2 (\sigma^2 + \zeta^2) + k_1 (\sigma^2 + \zeta^2)^2 + k_2 \left(\frac{\sigma^4}{2} + \zeta^4 \right) + k_3 \chi \sigma^2 \zeta \\ &\quad - k_4 \chi^4 - \frac{1}{4} \chi^4 \ln \frac{\chi^4}{\chi_0^4} + \frac{\delta}{3} \ln \frac{\sigma^2 \zeta}{\sigma_0^2 \zeta_0} . \end{aligned} \quad (3)$$

An explicit symmetry breaking term mimics the QCD effect of non-zero current quark masses

$$\mathcal{L}_{\text{SB}} = - \left(\frac{\chi}{\chi_0} \right)^2 \left[m_\pi^2 f_\pi \sigma + (\sqrt{2} m_K^2 f_K - \frac{1}{\sqrt{2}} m_\pi^2 f_\pi) \zeta \right] . \quad (4)$$

Finally, there are leptonic contributions from electrons and muons

$$\mathcal{L}_{\text{lep}} = \sum_{l=e,\mu} \bar{\psi}_l [i\gamma_\mu \partial^\mu - m_l] \psi_l . \quad (5)$$

\mathcal{L}_{kin} in (1) contains the kinetic energy terms of the hadrons. The general model incorporates the complete lowest baryon and meson multiplets. In the previous formulae we only

considered the degrees of freedom relevant for a neutron star calculation, the scalar field σ and its $s\bar{s}$ counterpart ζ (which can be identified with the observed f_0 particle), as well as the ω , ρ and ϕ vector mesons. \mathcal{L}_{vec} generates the masses of the spin-1 mesons through the interactions with spin-0 mesons. The scalar interactions \mathcal{L}_0 induce spontaneous chiral symmetry breaking. Another scalar, isoscalar field incorporated in the model, the dilaton χ simulates the breaking of the QCD scale symmetry and can be identified with the gluon condensate[13], for a longer discussion see [10]). The effective masses $m^*(\sigma, \zeta) = g_\sigma \sigma + g_\zeta \zeta$ of the baryons are generated through their coupling to the scalar fields, which attain non-zero vacuum expectation values due to the self-interactions \mathcal{L}_l [10]. As the field strengths change in nuclear and neutron matter, the effective masses of the baryon octet are shifted, too. The grand canonical thermodynamic potential of the system at zero temperature can be written as

$$\Omega/V = -\mathcal{L}_{\text{vec}} - \mathcal{L}_0 - \mathcal{L}_{\text{SB}} - \mathcal{V}_{\text{vac}} - \sum_i \frac{\gamma_i}{(2\pi)^3} \int d^3k [E_i^*(k) - \mu_i^*] - \frac{1}{3} \sum_l \frac{1}{\pi^2} \int \frac{dk k^4}{\sqrt{k^2 + m_l^2}}. \quad (6)$$

The chemical potentials for the baryons read

$$\mu_i^* = \sqrt{k_{F,i}^2 + m_i^{*2}} \quad , \quad \mu_i = b_i \mu_n - q_i \mu_e = \mu_i^* + g_{i\omega} \omega_0 + g_{i\phi} \phi_0 + g_{i\rho} \rho_0 \quad , \quad (7)$$

with b_i , q_i , and $k_{F,i}$ being the baryon number, charge, and fermi momentum of the i th species. The energy density and pressure are given by

$$\varepsilon = \Omega/V + \sum_{k=i,l} \mu_k \rho_k \quad (8)$$

$$P = -\Omega/V. \quad (9)$$

By extremizing Ω/V one obtains self-consistent equations for the meson fields in conjunction with demanding vanishing total charge and β equilibrium as the time scales involved allow for weak interactions to take place.

III. STELLAR EQUATIONS

In the case of the static neutron star we integrate the TOV equations[14]:

$$\frac{dP(r)}{dr} = -\frac{(\varepsilon+P)(4\pi r^3 P+m)}{r^2(1-Y(r))} \quad (10)$$

$$\frac{dm(r)}{dr} = 4\pi r^2 \epsilon(r) \quad , \quad (11)$$

where P and ϵ are the pressure and energy density of the nuclear matter. $m(r)$ is the gravitational mass of the star inside of the radius r and $Y(r) \equiv 2m(r)/r$. Starting with some initial values for P and ϵ , $P(r=0) \equiv P_c$ and $\epsilon(r=0) = \epsilon_c(P_c)$, with $m(0) = 0$ one can integrate equations (10) and (11) up to the point of vanishing pressure, which defines the radius R of the star. Here the specific model of nuclear matter enters via the equation of state $\epsilon(p)$. For the low-density tail of the EOS we use a standard parametrization for the crust of the star as discussed in [9].

Due to the rotation the star in general is deformed. Assuming axial symmetry the metric of the rotating star can be written as:

$$ds^2 = \exp(2\nu)dt^2 - \exp(2\lambda)dr^2 - \exp(2\mu) \left(d\theta^2 + \sin^2 \theta (d\phi - \omega dt)^2 \right) . \quad (12)$$

The metric functions μ, ν, λ depend on the radius r and the polar angle θ . If we set $\omega = 0$ we recover the standard Schwarzschild metric for the static star with the choice $\exp(2\mu) = r^2$, $\exp(2\lambda) = 1/(1 - Y(r))$. Because of the dragging of the local inertial frame $\omega(r)$ depends on the radius (but not to lowest order on the polar angle, see [12]) and is not equal to the rotational frequency Ω of the star. Following [12] and defining the difference of the frequency of the local frame and Ω as $\bar{\omega} \equiv \Omega - \omega$ demanding equilibrium between pressure, centrifugal and rotational forces in the local frame the differential equation for the metric functions follows[12]

$$\frac{d}{dr} \left[j(r) \frac{d\bar{\omega}}{dr} + \frac{4}{r} j(r) \bar{\omega}(r) \right] = 0 \quad (13)$$

with $j = \exp(-\nu - \lambda)$. The rotation of the star generates a modification of the metric as shown in (12). Using a multipole expansion of the metric functions, one obtains corrections that up to quadrupole order read

$$\exp(2\nu) = \exp(2\phi) (1 + 2(h_0 + h_2 P_2(\cos \theta))) \quad (14)$$

$$\exp(2\mu) = r^2 (1 + 2(v_2 - h_2 P_2(\cos \theta))) \quad (15)$$

$$\exp(2\lambda) = \frac{1}{1 - Y(r)} \left(1 + \frac{2m_0 + m_2 P_2(\cos \theta)}{r(1 - Y(r))} \right) , \quad (16)$$

where the static metric component ϕ is given by

$$\frac{d\phi}{dr} = -(\epsilon + P)^{-1} \frac{dP}{dr} . \quad (17)$$

The monopole coefficients h_0 and m_0 obey the differential equations ($r < R$):

$$\frac{dm_0}{dr} = 4\pi r^2 \frac{\partial \epsilon}{\partial P} (\epsilon + P) p_0 + \frac{1}{12} j^2 r^4 \left(\frac{d\bar{\omega}}{dr} \right)^2 + \frac{8\pi}{3} r^4 j^2 \frac{\epsilon + P}{1 - Y} \bar{\omega}^2 \quad (18)$$

$$\frac{dp_0}{dr} = -\frac{1 + 8\pi r^2 P}{r^2 (1 - Y)^2} m_0 - 4\pi r \frac{\epsilon + P}{1 - Y} p_0 + \frac{1}{12} \frac{r^3 j^2}{1 - Y} \left(\frac{d\bar{\omega}}{dr} \right)^2 + \frac{1}{3} \frac{d}{dr} \left(\frac{r^2 j^2 \bar{\omega}^2}{1 - Y} \right) \quad (19)$$

$$h_0 = -p_0 + \frac{r^2}{3} \bar{\omega}^2 \exp(-2\phi) + h_0^c \quad . \quad (20)$$

The value h_0^c is fixed by requiring that $h_0(R) = -\frac{m_0(R)}{R(1-Y(R))}$ at the star's surface as can be inferred from the large- r asymptotics for $h_0(r)$ [15]. Here m_0 and p_0 are the monopole mass and pressure perturbation due to the rotation of the star. The first terms where the actual deformation of the star's shape show up are the quadrupole corrections h_2, m_2 and v_2 . They can be determined by solving [12, 15]

$$\frac{dv_2}{dr} = -2 \frac{d\phi}{dr} h_2 + \left(\frac{1}{r} + \frac{d\Phi}{dr} \right) \left\{ -\frac{r^3}{3} \frac{dj^2}{dr} \bar{\omega}^2 + \frac{j^2}{6} r^4 \left(\frac{d\bar{\omega}}{dr} \right)^2 \right\} \quad (21)$$

$$\begin{aligned} \frac{dh_2}{dr} = & h_2 \left\{ \frac{d\phi}{dr} + \frac{2}{1 - Y} \left[2\pi(\epsilon + P) - \frac{m}{r^3} \right] / \left(\frac{d\phi}{dr} \right) \right\} - \frac{2}{r^2 (1 - Y)} / \left(\frac{d\phi}{dr} \right) v_2 \\ & + \frac{r^3}{6} \left(j \frac{d\bar{\omega}}{dr} \right)^2 - \frac{1}{3} (r\bar{\omega})^2 \frac{dj^2}{dr} \left\{ r \frac{d\phi}{dr} + \left[2r(1 - Y) \frac{d\phi}{dr} \right]^{-1} \right\} \quad . \quad (22) \end{aligned}$$

Integrating the equations and ensuring the correct asymptotics of vanishing corrections at $r = 0$ and $r = \infty$ by adding the appropriate solution of the homogeneous equations one obtains the quadrupole corrections to the metric. The mass and pressure quadrupole corrections follow as [12]

$$m_2 = r(1 - Y) \left\{ \frac{r^4}{6} \left(j \frac{d\bar{\omega}}{dr} \right)^2 - \frac{r}{3} (r\bar{\omega})^2 \frac{dj^2}{dr} - h_2 \right\} \quad (23)$$

$$p_2 = -h_2 - \frac{r^2}{3} \exp(-2\phi) \bar{\omega}^2 \quad . \quad (24)$$

After determining the metrical components we can then calculate radii, masses and moments of inertia of the rotating solutions.

IV. NUMERICAL RESULTS

We use the same parameter set (called ‘‘C1’’ in [7, 10]) that was also used in calculations of excited nuclear matter and finite nuclei. Figure 1 shows the result of a calculation of

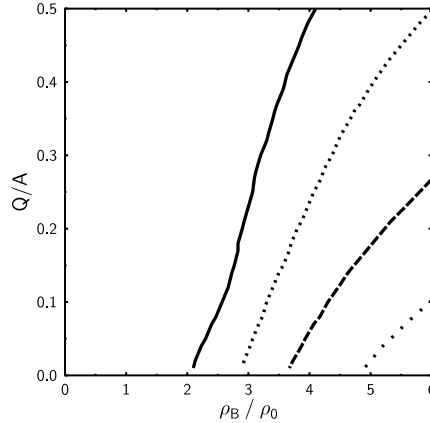


FIG. 1: Strangeness content of nuclear matter as function of charge per baryon and density. The full line shows the onset of strangeness in the system, the following lines mark the strangeness fraction $f_s = 0.1, 0.2$, and 0.3 respectively, where f_s is defined as number of strange quarks per baryon

nuclear matter varying the average charge of the system between symmetric nuclear matter ($Q/A = 0.5$) to neutral hadronic matter ($Q = 0$). One can see how the onset of hypermatter is shifted from neutral matter at a density of $\approx 2\rho_0$ to twice that value for symmetric nuclear matter. Note that here no leptons are taken into account that shift the total baryonic charge to positive values in the case of a neutron star. There, Λ and Σ states are populated at densities higher than $2.6 \rho_0$ [9]. Looking again only at the baryonic contributions Figure 2 shows the the energy per baryon $E/A - m_N$ as a function of density for total isospin per baryon (3rd component) zero and -0.5 . The isospin 0 curve exhibits the nuclear matter saturation properties. The thick solid line shows the result of the baryonic energy inside the neutron star (including leptons) as calculated in the chiral model. One can see that for higher densities the equation of state resembles more the isospin 0 nuclear matter results. In fact, in the extreme high-density limit assuming similar population of the baryonic octet the total isospin tends towards zero again.

The maximum frequency Ω_K and the minimum rotational periods $P_s \equiv 2\pi/\Omega_K$ of a rotating neutron star have been determined by integrating the self-consistent equation [15]

$$\bar{\omega} = V(\Omega) \exp[\nu(\Omega) - \mu(\Omega)] \quad (25)$$

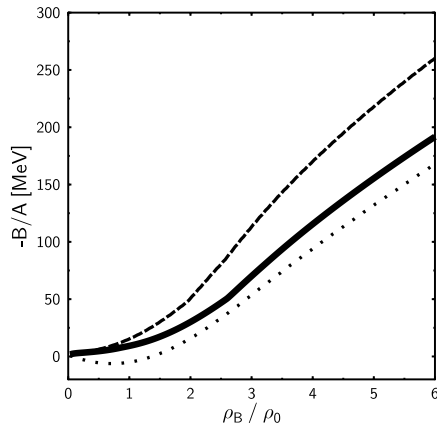


FIG. 2: Binding energy of nuclear matter as function of baryon density. The figure shows isospin symmetric matter (dashed line) and neutral baryonic matter including strange baryons (solid line).

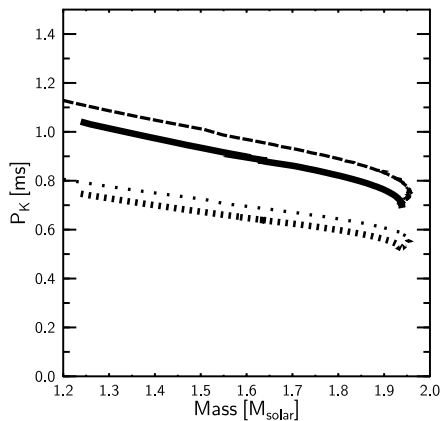


FIG. 3: Minimum rotational periods P_K for stars with different central energy density. The upper two curves are results for the chiral model (full line) and the TM1 relativistic mean field model. The lower curves are the corresponding Newtonian estimates.

solving for Ω at the equator of the star, where the mass shedding occurs first, for different central energy densities and total masses of the star. The resulting values are shown in Figure 3. Compared to the Newtonian value of the Kepler period (dashed lines) there is an increase in P_K of about 25% due to the general relativity corrections. This result is in accordance with other calculations of different neutron star models, which show similar

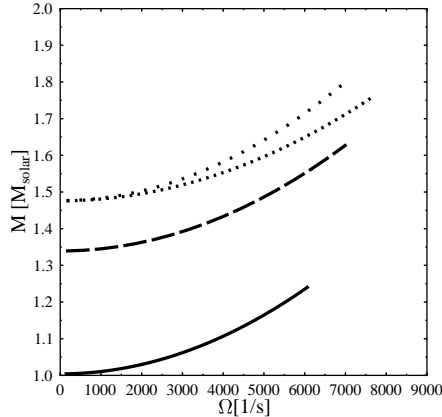


FIG. 4: Mass of different neutron star as function of rotational frequency. The sharply rising dotted curve show a result for the TM1 parameterization.

results [16]. In the plot also results for a relativistic mean-field parametrization (TM1 [11]) are shown, which was extended to include hyperons (see [9]). The difference of the Kepler frequency for both parameterizations is small. Note that the maximum gravitational mass of the neutron star that was about $1.64 M_{\odot}$ in case of the static solution [9] is now increased to 1.94 solar masses due to the additional rotational contribution. Looking at the frequency dependence by spinning up the neutron star one gets the increasing neutron star mass as shown in Figure 4. One TM1 result for a star with $M(\Omega=0) = 1.48M_{\odot}$ is shown for comparison. In this case one can see a distinctly sharper rise of the mass of the star with rotational frequency. For the chiral case one can observe the increase of the mass by up to 30% at the mass-shedding frequency.

Similarly looking at the monopole corrections one can calculate the increase of the radius of different star solutions due to rotation averaged over the star's surface. Figure 5 shows that there is an increase of the radius by up to 10% close to Ω_K . Again, the TM1 model shows a more drastic change with rotation. From calculating the quadrupole coefficients Eqs. (16) one can determine the excentricity ϵ_{ex} of the star defined via the ratio of the surface radius at the equator over the pole radius:

$$\epsilon_{ex} = \sqrt{1 - R_{pole}^2/R_{equator}^2} \quad (26)$$

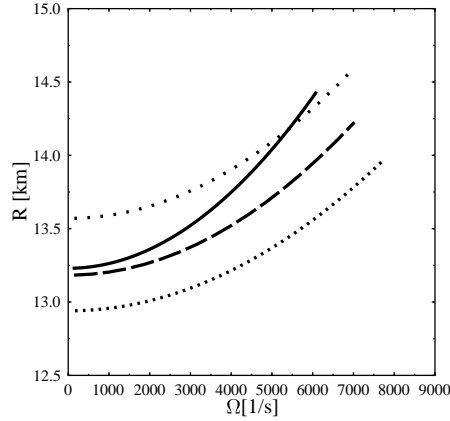


FIG. 5: Radius of different neutron star (cf. Fig. 4) as function of rotational frequency.

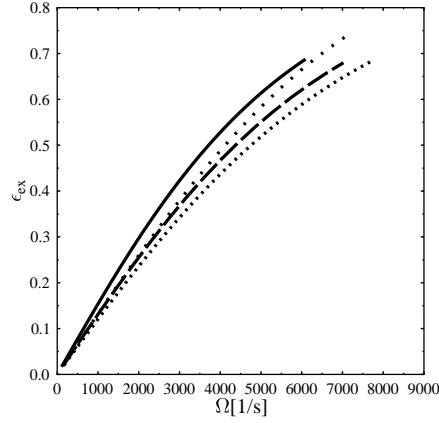


FIG. 6: Excentricity of the deformed rotating neutron star as function of rotational frequency.

Figure 6 shows that there is a substantial deformation of the star. This has also an impact on the internal structure of the star depending on the polar angle. This is shown in Figure 7. Here the onset of the various hyperons contained in the star Σ^- , Λ and Ξ^- are shown for a typical static star with a Mass of $1.475 M_\odot$ (vertical lines) compared to the same solution corrected for rotational effects at its Kepler frequency.

Integrating the inertia of the star by using the general expression [16]

$$I = 2\pi \int d\theta dr \exp\{\lambda + \mu + \nu + \psi\} (\epsilon + P) \left(\exp[2\nu - 2\psi] - \bar{\omega}^2 \right) \frac{\bar{\omega}}{\Omega} \quad (27)$$

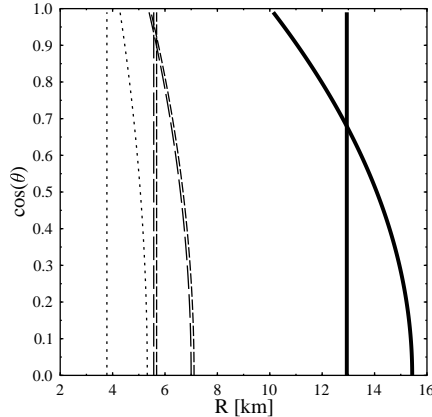


FIG. 7: Inner structure of the neutron star. The onset of hyperon population in the interior of the neutron star as function of depth and polar angle is shown for Λ (long-dashed lines), Σ^- (dashed lines) and Ξ^- particles (dotted lines) is shown. The full line represents the star's surface. For comparison the thresholds and the radius for the corresponding static star are shown (straight lines).

and again taking into account the corrections to the metric up to order Ω^2 one gets the moment of inertia of the star as shown in Fig. 8. In this case the mass of the non-rotating star is 1.48 solar masses. In this figure we have kept the baryonic number of the star constant at $M_B = 1.22 \cdot 10^{57} \sim (M_B)_{solar}$ and changed the rotational frequency. The curve therefore shows the change in the moment of inertia during the spin-down of a pulsar, the energy-loss of the star generated by electromagnetic and gravitational radiation. Assuming a simple power-law of the energy loss $\Delta E \sim -E_o^{n_o}$ where $n_o = 3$ and $n_o = 5$ in the case of magnetic and gravitational radiation, respectively. With this assumption one can determine the frequency-dependent braking index $n(\Omega) = n_o - \Delta n(\Omega)$ with

$$\Delta n = \frac{3I'\Omega + I''\Omega^2}{2I + I'\Omega} \quad (28)$$

where the prime denotes the derivative with respect to frequency. Figure 9 shows the shift of the braking index. There is a substantial reduction in the case of fast rotating stars that has to be taken into account for an analysis of the time evolution of the star. However, one cannot see significant structures as for instance a back-bending shape as seen in moments of inertia of atomic nuclei and also suggested for neutron stars[17]. This is not very surprising,

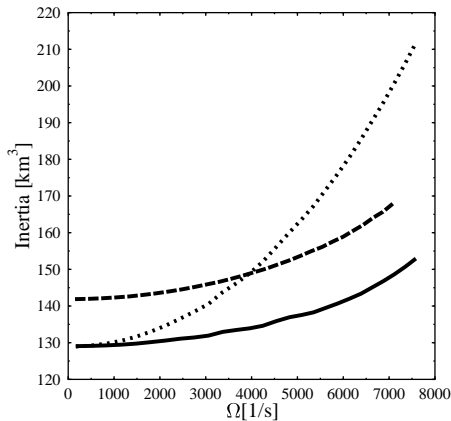


FIG. 8: Moment of inertia of the rotating star as function of frequency. A fixed value of M_B is assumed. The result of the chiral model (solid line), the TM1 calculation (dashed lines) and in comparison the inertia of the star neglecting the deformation (dotted line) in the case of the chiral model are shown.

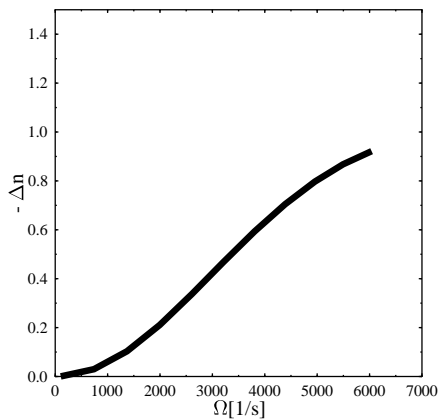


FIG. 9: Deviation of the braking index from an assumed power law. In the case of magnetic radiation the index is reduced by a factor of up to $1/3$.

since the chiral model does not show a phase transition for low temperatures and at high densities (see, however, the discussion in the concluding section). Note that in this case at maximum rotation the star starts with a central density of 2.3 times nuclear matter density, which is below the threshold of the occurrence of hyperons. Below a frequency $\Omega \sim 5600/\text{s}$

($P \sim 1.1\text{ms}$) hypermatter becomes energetically more favorable.

V. CONCLUSION

We have used a chiral SU(3) model for the calculation of rotating neutron stars. The model parameters have been fitted to reproduce hadronic masses and saturation properties of groundstate nuclear matter. Within the same model and with the same parameters also nuclei and hypernuclei have been described quite successfully. The resulting star shapes show a significant excentricity which can also be seen from its hypermatter distribution in the interior of the star. The moment of inertia shows a rather strong dependence on the rotational frequency, which has to be taken into account for analyzing the spinning-down and related age-estimates of pulsars. No back-bending of the inertia occurs due to the lack of a phase transition of the chiral model for high densities and low temperatures. In general the comparison with a quite different model that contains hyperons shows the robustness of the results for the rotating star as well as the relative insensitivity of the star properties on very different models with quite distinct hyperon content[9]. In this context a discussion of the possible effects of populating higher baryonic resonances in the neutron star should be performed. Those additional degrees of freedom can change the high-density behavior of the system significantly, generating a different structure of the time-evolution of the rotating star. Such a calculation might rule in or out specific theoretical descriptions of hadronic resonances by studying their effect on neutron star properties. Work in this direction is in progress [18].

Acknowledgments

This work was supported in part by the U.S. Department of Energy, Nuclear Physics Division (Contract No. W-31-109-Eng-38). The authors thank M. Hanauske and S. Pal for valuable discussions.

[1] N.K. Glendenning, *Compact Stars* (Springer, New York, 1997).

[2] D. Bhattacharya and E. P. J. van den Heuvel, Phys. Rep. 203, 1 (1991).

- [3] E. J. Groth, *Astrophys. J. Suppl.* 29, 453 (1975).
- [4] A. G. Lyne, R. S. J. Pritchard, and F. Graham-Smith, *Nature* 381, 497 (1996).
- [5] R. Manchester, J. Durdin, and L. Newton, *Nature* 331, 374 (1985).
- [6] e.g. Ch. Gouiffes, J. P. Finley, H. Ögelman, *Ap. J.* 394, 581 (1992).
- [7] D. Zschesche, P. Papazoglou, S. Schramm, J. Schaffner-Bielich, H. Stöcker, W. Greiner, *Phys. Rev. C* 63, 025201 (2001).
- [8] Ch. Beckmann, P. Papazoglou, S. Schramm, D. Zschesche, H. Stöcker, W. Greiner, *Phys. Rev. C* 65, 024301 (2002).
- [9] M. Hanauske, D. Zschesche, S. Pal, S. Schramm, H. Stöcker, and W. Greiner, *Ap. J.* 537, 958 (2000).
- [10] P. Papazoglou, D. Zschesche, S. Schramm, J. Schaffner-Bielich, H. Stöcker, and W. Greiner, *Phys. Rev. C* 59 (1999) 411.
- [11] Y. Sugahara and H. Toki, *Nucl. Phys. A* 579, 557 (1994).
- [12] J. B. Hartle and K. S. Thorne, *Ap. J.* 153, 807 (1968).
- [13] J. Schechter, *Phys. Rev D* 21 (1980) 3393.
- [14] R.C. Tolman, *Phys. Rev.* 55 (1939) 364;
J.R. Oppenheimer and G.M. Volkoff, *Phys. Rev.* 55 (1939) 374.
- [15] F. Weber, *Pulsars as Astrophysical Laboratories for Nuclear and Particle Physics*, IoP Publishing Bristol, Chapter 15 (1999).
- [16] F. Weber and N. K. Glendenning, *Ap. J.* 390, 541 (1992).
- [17] N. K. Glendenning and F. Weber, *Phys. Rev. Lett.* 79, 1603 (1997).
- [18] S. Schramm and D. Zschesche, in preparation.